[1]Avinash Kumar,

[2]Dr. Anil Kumar

Optimization of Energy Balances of a Photovoltaic Power Plant with Electrochemical and Thermal Storage of Solar Energy

Journal of Electrical Systems

Abstract*:* - In this paper, the optimization of a solar photovoltaic thermal (PV/T) water collector which is based on energy concept is carried out. Considering energy balance for four different season components of PV/T collector, we can obtain analytical expressions for thermal parameters (i.e. solar cells temperature, outlet water temperature, useful absorbed heat rate, average water temperature, mass, etc.). The simulation results are in good agreement with global solar irradiance data ,greywolf has been used to optimize the energy balance of PV/T water collector. Massive PV introduction induces difficult power supply-demand balance adjustment. As one of solutions, a PV system and a Solar Hot-Water Supply System which is a hybrid system of a Solar Thermal Water Heater and a Heat Pump Water Heater are combined. In optimization of these configuration, it is necessary to consider the optimization of multiple objectives such as cost and energy efficiency. However, it is difficult to satisfy these objectives simultaneously since these are trade-offs. In this paper, we conducted to find optimal solutions by greywolf Optimization which is a kind of an evolutionary computing. To facilitate the solution search within the constraints conditions, optimal solutions according to each objective, and conducted a search twice for solutions by greywolf Optimization with fixed configuration to find better solutions with respect to operation. As a result, the evaluation values of all objective functions are improved.

Keywords*:* Photovoltaic–Thermal (PV/T) Collector,Hybrid Solar Energy System,Thermal Parameter Analysis,Solar Cell Temperature,Outlet Water Temperature,Energy Balance Optimization. Rey Wolf Optimizer (GWO)

1.INTRODUCTION

Nowadays using renewable energies is considered more because of fossil fuels high price and the environmental problems which are caused by them. One of an abundant renewable energy sources is solar energy. The electrical efficiency of PV system decreases as a result of decrease in electrical voltage. In a solar collector system, an external electrical source is needed to circulate the agent fluid through the system. Therefore, if we combine a PV module and a solar collector system, the electrical source can be provided for solar collector system. On the other hand, the additional heat which is absorbed from PV module causes solar cells temperature to decrease and as a result electrical efficiency increases.[1] Combining these two systems, we can also use optimum installation space. Using a PV/T collector, we can convert solar energy in to electricity and heat. As we know, the quality of these two kinds of energies is not the same. Using energy analysis, we can compare these two kinds of energies, which are different in their quality. Using energy optimization, we can determine optimum operating mode of PV/T water collector[2]

Coupling solar energy and storage technologies is one such case. The reason: Solar energy is not always produced at the time energy is needed most. Peak power usage often occurs on summer afternoons and evenings, when solar energy generation is falling. Temperatures can be hottest during these times, and people who work daytime hours get home and begin using electricity to cool their homes, cook, and run appliances. Storage helps solar contribute to the electricity supply even when the sun isn't shining.[4]It can also help smooth out variations in how solar energy flows on the grid. These variations are attributable to changes in the amount of sunlight that shines onto photovoltaic (PV) panels or concentrating solar-thermal power (CSP)

[1]Research scholar, Electrical Engineering Department
IFTM University, Moradabad
[2]Supervisor, Head of Department, Electrical Engineering Department
IFTM University, Moradabad

systems. Solar energy production can be affected by season, time of day, clouds, dust, haze, or obstructions like shadows, rain, snow, and dirt. Sometimes energy storage is co-located with, or placed next to, a solar energy system, and sometimes the storage system stands alone, but in either configuration, it can help more effectively integrate solar into the energy landscape.[5-6]

To harmonize the energy balance of a stand-alone photovoltaic system, electrochemical batteries are widely used for that purpose. They are providing storage and exchange of electricity for the target of guaranteed power supply to consumers. Unfortunately, batteries have a limited operating lifetime, they are sensitive to operating temperature and have a high cost. Typical stand-alone electrification examples are small villages and farm facilities. [7]Among the electrical receivers of such consumers, a significant proportion is occupied by electric heaters. According to [5], the minimum daily consumption rate of hot water per human in a private house is 20~30 liters. Technological needs for milking one cow on dairy farms require an average of 24 to 28 liters of hot water per day [6]. For the consumers of the power supply under consideration, the accumulation of electricity of photovoltaic cells can be carried out not only in electrochemical batteries but also in water-heating installations.[8] These installations will make it possible to reduce the cost of a photovoltaic power plant by reducing the capacity of batteries. There are a large number of solar water heaters, characterized by simplicity of design and low cost[8] The specific cost of collectors of various designs differs by an order of magnitude. The simplest solar collectors cost from 2.3 thousand rubles/m2.[9] Such collectors have an efficiency of about 19%. The most advanced evacuated tubular collectors cost already 25 thousand rubles/m2 , which far exceeds the specific cost of photovoltaic panels. The efficiency of such collectors reaches 51-57% [10]

2.RELATED STUDY

Thermal Energy Storage-Thermal energy storage is a family of technologies in which a fluid, such as water or molten salt, or other material is used to store heat. This thermal storage material is then stored in an insulated tank until the energy is needed.[11] The energy may be used directly for heating and cooling, or it can be used to generate electricity. In thermal energy storage systems intended for electricity, the heat is used to boil water. The resulting steam drives a turbine and produces electrical power using the same equipment that is used in conventional electricity generating stations. Thermal energy storage is useful in CSP plants, which focus sunlight onto a receiver to heat a working fluid. Supercritical carbon dioxide is being explored as a working fluid that could take advantage of higher temperatures and reduce the size of generating plants.[12].Proposed an integrated optimization framework for PV-TEG systems combining PV optimization, TEG enhancement and advanced cooling strategies. Experiments show that coordinated cooling and PV control significantly improve overall system efficiency under varying solar conditions.[13]Developed a hybrid PV–heat pipe–TEG–radiative cooling system and validated it in COMSOL. The combined passive cooling reduced PV temperature by 2–13°C and improved efficiency by up to 1.8%, with significant gains in harsh climates like deserts.[14]Compared active and hybrid (TEG + PCM) cooling for PV systems. The hybrid system maintained stable PV temperature for 4 hours and improved efficiency by 2.5–3.5% and power generation by 20–30%, showing strong temperature-regulation capability.[15]Presented a CPV + two-stage TEG cogeneration model including Seebeck, Peltier and Thomson effects. The integrated system achieved ~8% higher power density and efficiency compared to standalone CPV and revealed key design parameters influencing hybrid performance.[16]Reviewed technological advances in solar thermoelectric generators (STEG) and PV-TEG hybrids, discussing efficiency limits, material challenges, PV losses and integration approaches. Emphasizes future potential with high-ZT materials and optimized hybrid architectures.[17]Explored thermoelectric modules for PV cooling and cogeneration in building-integrated systems. Findings show that TEMs can enhance PV efficiency significantly, with future adoption depending on advanced thermoelectric materials and improved system designs.[18]

Dataset

The Global Solar Atlas online app (https://globalsolaratlas.info/), prepared by Solargis under contract to The World Bank, based on a solar resource database that Solargis owns and maintains. It provides the estimated solar resource, air temperature data and potential solar power output for the selected location and input parameters of a photovoltaic (PV) power system.[[19]

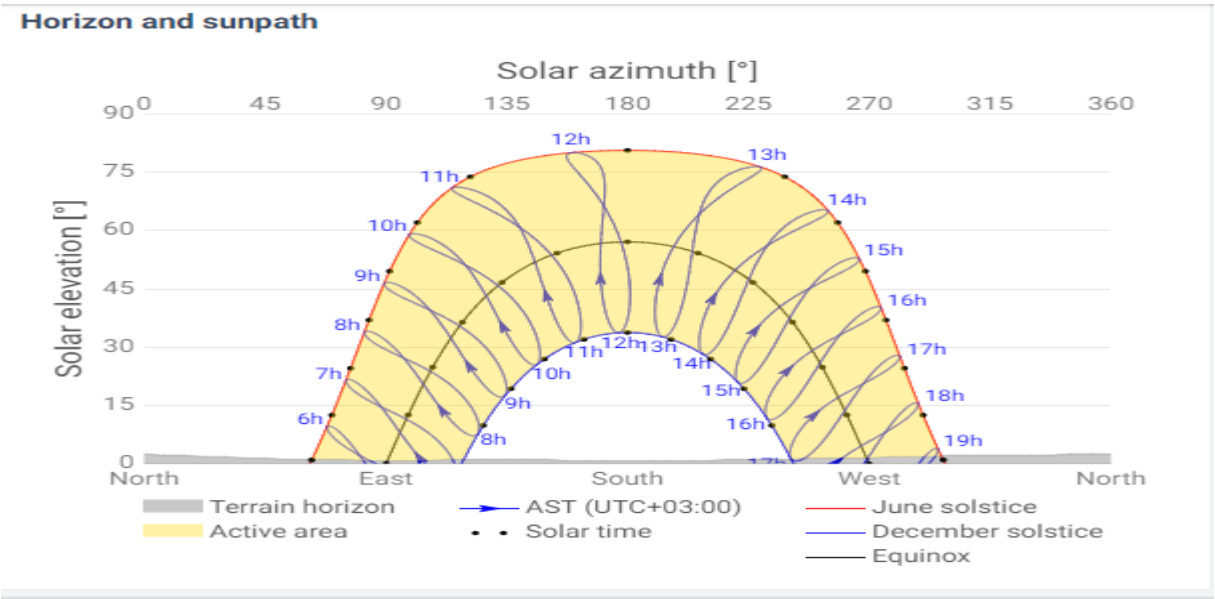

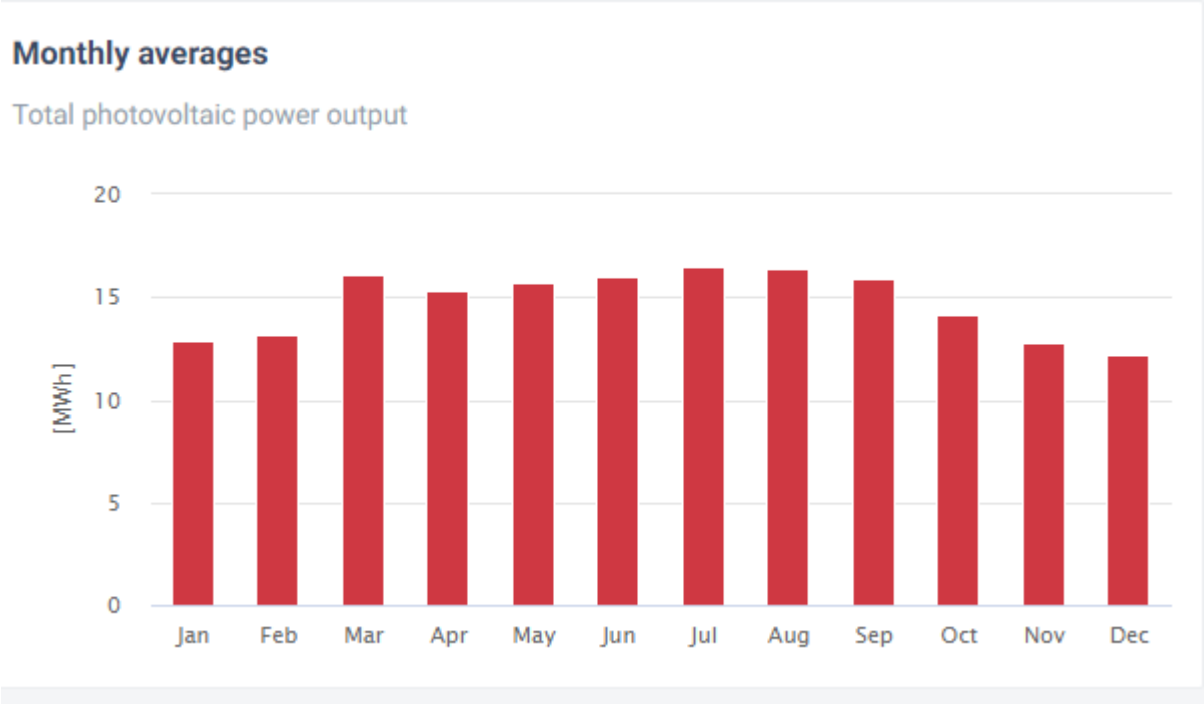

Object of the research. Potential objects of electrifications from power plants of renewable energy are the following Optimization of energy balances of a photovoltaic power plant with electrochemical and thermal storage of solar energy the characteristics of the combined electricity storage of a photovoltaic power plant that supplies a private house. Energy needs at home can be evaluated as the sum of electricity consumption determined by social requires. They are the following: an average of 70 kWh per human per month [20-23], which is 2.3 kWh per day, or 7~9 kWh per family of 3~4 people including additional electricity consumption on hot water. Energy costs for heating water can be determined by the formula [24]:

$$P_t = m \,.C_{w.}\,(Q_2 - Q_1)\; t\; w = \cdot\cdot - (1)$$

where t – a time of heating water [s], P is the power of the heating element [kW], m is the mass of water [kg], Cw (4.2 kJ/kg·deg) – specific heat capacity of water, Q2 and Q1 – the final and initial temperature of the water. With an initial water temperature of 10 Celcius degrees, the daily energy demand of a water heater for heating 60~80 liters of water to 50 Celcius degrees will be about 10~13 kWh. The total daily power consumption of the house for the considered example will be:

$$W = W_{e+} W_{sh}$$

where We – is the electricity consumed by electrical loads, Wwh – the electric power consumed by the water heater. This amount of electricity must be generated daily by a photovoltaic power plant, and the necessary amount of this energy must be supplied to the electric receivers through the storage systems.[25]

3.PROPOSED SYSTEM

The proposed system is a hybrid solar–thermal power-supply microgrid that combines a photovoltaic–thermal (PVT) plant with wind generation, a small hydroturbine, a battery energy-storage system and the utility grid. All generators are connected to a common AC bus and are coordinated so that the varying 24-hour electrical demand is met with minimum operating cost and reduced dependence on the utility grid.Solar energy is captured through the detailed hybrid_solar_thermal Simulink model. The PV part converts irradiance into electrical power, while the thermal part recovers heat for useful thermal demand, as described in the previous section. The PV array has a rated power of 60 kW and its output depends on the irradiance and temperature profiles generated inside the script. In parallel, a wind turbine produces electrical power as a function of the stochastic wind-speed profile $v_{wind(t)}$ bounded by a maximum wind power WTpmax=100.

A hydroturbine provides dispatchable renewable power up to pHT,max=50 kW, with realistic operating constraints such as minimum up/down times, start-up costs and water-flow–related cost coefficients. These constraints are reflected in parameters like the minimum up time (600 s), minimum down time (300 s), hot and cold start-up times and the water-consumption and operating-cost coefficients.To smooth the mismatch between renewable generation and load, the system includes a battery energy-storage system. The battery has a nominal voltage of 108 V, a rated capacity of 26 Ah and is operated within specified charging and discharging power limits (1000 W≤PBATT≤16000 W)

with round-trip efficiency ηBATT=0.9.Its state of charge (SoC) is tracked over the 24-hour horizon and the script enforces admissible charging/discharging power bounds BATTpmin,BATTpmax.When the combination of PV, wind, hydro and battery cannot fully satisfy the time-varying load profile (ranging roughly from 650 kW to 1.12 MW as defined in p_bus(index_Load,:)), the deficit is supplied by the utility grid, modeled as an additional source with unit energy price =1.05 $/kWh.

The overall power-management problem is formulated as a short-term economic dispatch over 24 one-hour intervals. For each hour the decision variables are the hydroturbine output, the battery charging/discharging power and the power drawn from the grid. The cost function aggregates the operating costs of the hydroturbine (water-usage cost and start-up cost), the wind and PV generation costs, and the energy purchased from the utility. This optimization is solved using the Grey Wolf Optimizer (GWO). First, initial_wolf constructs a candidate population of schedules based on the forecast wind, PV power and load, together with the current battery SoC and hydroturbine status. Then greywolffunction iteratively updates these candidates (the “wolves”) to minimize total cost while respecting all power limits and operating constraints. The best schedule yields optimized hourly set-points for hydroturbine power (gb_mt), battery power (gb_batt) and grid power (gb_util), which are written back to the power-bus matrix p_bus and used to simulate the final system performance

System Implementation

Let the operating horizon be divided into equal time steps:

- t∈ T = {1.2. ……T}- time index (e.g. hours in a day or year).
- Δt- duration of each time step [h]

PVT Generator Module: Electrical and Thermal Model

Parameters

- A_{pvt-}aperture area of one PVT module [M^2]
- N_{pvt-}number of PVT modules in the field
- G (t) solar irradiance incident on the PVT plan[W/M^2]
- $T_{\propto}$ambient temperature [\!^\circ\text{C}]
- $\eta e, ref$ −PVelectrical efficiency at reference temperature T_{ref}
- β −PV –temperature coefficient [1/K]
- U_{L-}- overall heat-loss coefficient of the PVT collector [W/(m2\cdotpK)]
- (τα)- effective transmittance–absorptance product of the PVT absorber
- m˙f mass flow rate of heat-transfer fluid per string [kg/s]
- cp,f specific heat of the heat-transfer fluid [J/(kg\cdotpK)].

Electrical Submodel

PV cell temperature is approximated as:

$$\boldsymbol{T_c(t) = T_{\propto} + k\ G(t)}$$

where κ is an empirical coefficient,Temperature-dependent electrical efficiency:

$$\boldsymbol{\eta_e(t) = \eta_{e,ref[1-\beta(T_c(t))-T_{ref}]}}$$

Electrical power from the PVT field:

$$\boldsymbol{P_{pV}(t) = N_{pvt}A_{pvt,}\eta_e(t)G(t)}$$

This is the DC-side PV power before converters.

Thermal Submodel

Useful thermal power extracted by the fluid (per field):

$$\boldsymbol{Q_u(t) = m_f c_{pf,}(T_f^{out}(t)\text{-}\ T_f^{in}(t))}$$

Mean fluid temperature:

$$\boldsymbol{T_m(t) = \frac{T_f^{out}(t) - T_f^{in}(t)}{2}}$$

Flat-plate energy balance:

$$\boldsymbol{Q_u(t) = U_{L,}[(t\alpha)G(t) - U_L(T_m(t) - T_{\propto}(t))]}$$

Energy balance of the PVT module:

$$N_{pvt}A_{pvt}\ G(t) = p_{pv}(t) + Q_u(t) + Q_{loss,pvt}(t)$$

with

$$Q_{loss,pvt}(t) = U_L N_{pvt} A_{pvt}(T_m(t) - T_\propto(t))$$

Power Conditioning and Inverter

Let

- η_{dc-} efficiency of DC/DC converter with MPPT
- η_{inv-} inverter efficiency

AC-side PV power injected to the AC bus

$$P_{PV,AC}(t) = \eta_{dc}\ \eta_{dc-} P_{PV}(t)$$

This energy is available for **AC loads, battery conversion (if DC-coupled) and grid export**.

Battery Energy Storage System (BESS)

Parameters

- $E_{bat,max}$ − nominal capacity of the battery [kWh]
- SOC(t) −state of charge (fraction 0–1)
- $\eta_{ch.}\eta_{dic}$ − charge and discharge efficiencies
- $P_{ch,max,}P_{dis,max}$ − rated charge and discharge power.

Decision Variables

- $P_{ch,}(t) \geq 0$ – battery charging power [kW]
- $P_{ch,max,} \geq 0$ – battery charging power [kW]

SOC Dynamics

Stored energy:

$$E_{bat,}(t) = SOC(t)\ E_{bat,max}$$

SOC update:

$$SOC(t+1) = SOC(t) + \frac{\eta_{ch} P_{ch} \Delta t}{E_{bat,max}} - \frac{P_{dis}(t) \Delta t}{\eta_{ch} E_{bat,max}}$$

Constraints:

$$SOC_{min,} \leq SOC(t) SOC \leq SOC_{max,}$$

$$0 \leq P_{ch,}(t) \leq P_{ch,max,}\ 0 \leq P_{dis}(t) \leq P_{dis,max,}$$

Thermal Storage Module

Parameters

- $M_{st,}$ −mass of storage medium (e.g. water) [kg]
- $c_{p,st}$ − specific heat [J/(kg\cdotpK)]

- $T_{st,}(t)$ – average storage temperature [\!^\circ\text{C}]
- $T_{ref,}$ – reference temperature (e.g. cold inlet)
- $U_{st,}$ –storageheat-losscoefficient [W/(m^2\cdotpK)]
- $A_{st,}$effective external area of tank [m^2]

Decision Variables

- $Q_{ch,th}(t) \geq 0$ – heat sent from PVT field to storage [kW][\text{kW}][kW]
- $Q_{dis,th}(t) \geq 0$ – heat supplied from storage to thermal load [kW]

Stored Energy and Dynamics

- Stored thermal energy:

$$E_{th,}(t) = \frac{M_{st}\, C_{p,st}}{3600}\ (T_{st,} - T_{ref,})\ [kWh_{th}]$$

Thermal loss:

$$Q_{loss,th}(t) = Q_{st,}\, A_{st,}(T_{st,}(t) - T_{\infty,}(t))$$

Energy balance (discrete):

$$E_{th,}(t+1) = E_{th,}(t) + (Q_{ch,th}(t) - Q_{dis,th}(t) - Q_{loss,th}(t))\,\Delta t$$

Constraints:

$$0 \leq E_{th}(t) \leq E_{th,max,}$$

$$0 \leq Q_{ch,th}(t) \leq Q_u(t),\ 0 \leq Q_{dis,th}(t) \leq Q_{loss,th}(t)$$

6. Grid Connection and Load Models

Parameters

- $p_{load,et}(t)$ – electrical demand profile [kW]
- $Q_{load,th}(t)$ – thermal demand profile [kW$_{th}$]
- $c_{el}(t)$ –grid electricity purchase tariff [₹/kWh]
- $c_{exp}(t)$ – feed-in tariff for exported power [₹/kWh]
- Q_{aux} – cost of auxiliary thermal energy [₹/kWth]

Decision Variables

- $P_{grid,imp}(t) \geq 0$ – grid import power [kW]
- $P_{grid,exp}(t) \geq 0$ – grid export power [kW]
- $Q_{aux,}(t) \geq 0$ – auxiliary heater output [kW$_{th}$]

Electrical Energy Balance

At each time ttt, on the AC bus:

$$P_{PV,AC}(t) + P_{grid,imp}(t) + P_{dis}(t) = p_{load,et}(t) + p_{ch,}(t) + P_{grid,exp}(t)$$

Thermal Energy Balance

On the thermal side:

$$Q_u(t) + Q_{dis,th}(t) + Q_{aux}(t) = Q_{load,th}(t) + Q_{ch,th}(t) + Q_{loss,th}(t)$$

Optimization Objective

A typical objective for your "Optimization of Energy Balances" is to **minimize the total operating cost** (electricity imported + auxiliary heat cost − revenue from export) over the horizon:

$$\text{Min } J = \sum_{t\in T}[c_{el}(t)\ P_{grid,imp}(t) - c_{exp}(t)\ P_{grid,exp}(t) + c_{aux}Q_{aux}(t)]\ \Delta t$$

- All module dynamics (PVT, battery, thermal storage)
- Electrical and thermal balance equations
- SOC and energy bounds
- Power and heat capacity limits.

GWO

An approach which is used for optimization and inspired by nature is known as GWO. In this approach gray wolves mechanism is discussed, on the basis of which they hunt prey. Four categories of gray wolves: ω, δ, β and α. In 2014, Mirjalili proposed this approach which pretends the hierarchy of gray wolves based on leadership. Four types of gray wolves are used to employ hierarchal leadership. Mechanism of hunting has been divided: 1. prey recognition, 2. prey bordering and 3. attack on prey. The important ability of gray wolves is that, first, they recognize their prey location and then encircle that prey. Therefore, the four types of gray wolves participate in hunting occasionally. We initialize α, β, δ and ω using a specified some value for smart appliances. A population Np is generated randomly To achieve optimization, GWO algorithm uses a mathematical model that represents the hunting behavior of grey wolves. The grey wolves surround their prey by making a circle as shown in fig. 1, the mathematical equations representing this encircling behavior are proposed in the paper Grey Wolf Optimizer. The equations are:

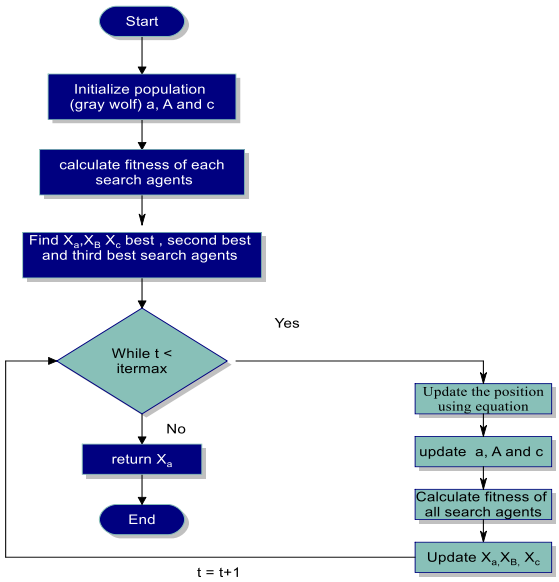

Figure 1 GWO Architecture

$$\overrightarrow{D} = |(\vec{C} .(\vec{X}_P(t)- (\vec{X}(t) |$$

$$\vec{X}(t+1) = \overrightarrow{X_P}(t) -\vec{A} .\vec{D}$$

$$\overrightarrow{A} = 2\vec{a}.\overrightarrow{r_1}-\vec{a}$$

$$\vec{C} = 2.\overrightarrow{r_2}$$

where t is the current run, A and C are coefficient vectors, Xp is the position vector of the prey, and the position vector of a grey wolf is indicated by X. Components of a are linearly decreased from 2 to 0 over the course of iterations and r1, r2 are random vectors in [0, 1].

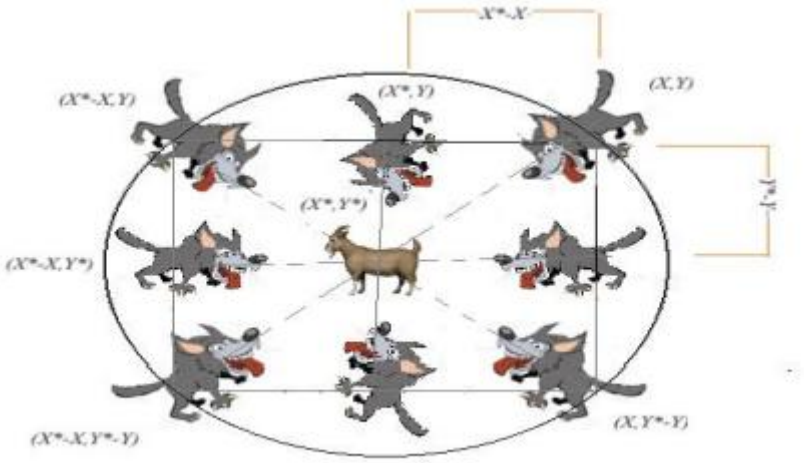

In the beginning, the wolves are positioned at random locations with reference to the location of the prey and further value of fitness function is computed for various random locations of wolves; consequently alpha, beta, gamma, delta solutions are taken note of. Throughout the simulation of GWO, the iteration apprises in the locations of all the grey wolves is depicted in Fig.2. Fitness function is reliant on distance assessment amongst the prey and the various wolves. The distance evaluated acts as a decisive factor in finding out the optimized solution determined by fitness function i.e. the wolf that is found to be nearest in location to the prey; has the higher probability of continuing to be closest to the prey in near future's time. Fig.2 illustrates the repeated iterations solution's as depicted by the alpha, beta, gamma and delta wolves. Algorithm1 exemplifies Grey Wolf Optimization. The GWO has been represented by the following equation (5, 6, and 7) and Fig. 2:

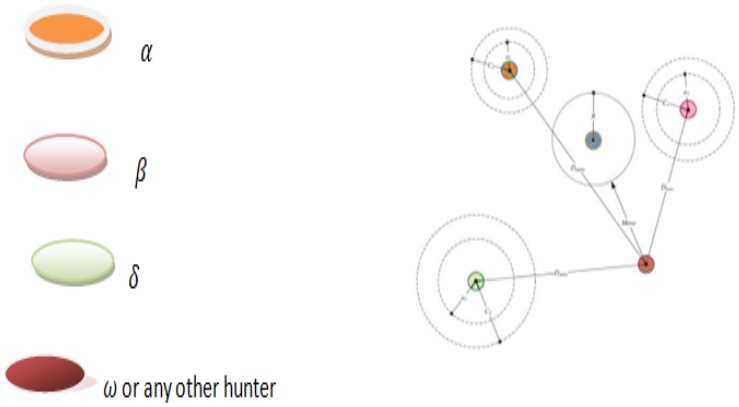

Algorithm 1: Traditional Grey Wolf Optimizer (GWO)

Input: Complex engineering problems having objective functions, constraints and decision

Variables.

Output: Search agent having the best solution.
1. Initialize the grey wolf population, a, A and C
2. Calculate the fitness of each search agents
3. Find Xα, ,X??, Xδ: best, second best and third best search, agents
4. while t < Itermax:
a. Update the position using equation (7)
b. Update a, A and C
c. Calculate the fitness of all search agents
d. Update Xα, X??, Xδ
e. Increment t by 1.
5. Return Xα
6. End.

4.RESULTS AND DISCUSSION

The electrical output power of a PV module depends primarily on the solar radiation energy (irradiation) being absorbed and transformed. To some extent the output power also depends on the actual operating temperature. With an increase of module temperature, output power decreases typically by 0.2%/°C0.5%/°C. The Sun's irradiance is only partially converted into electrical energy, one part of the module reaching irradiance is reflected back from the surface of PV module and the remaining part continues its way through the front layers of the module until it reaches the active semiconductor layer. If the module is transparent, transmitted component of the radiation is also present. Under realistic conditions, reflective losses are around 10% of the incoming irradiance, in the case of perpendicular incidence [9]. Furthermore, only one part of the absorbed radiation is converted to electrical energy, while the rest is converted into heat. The PV module output electrical power is determined by module efficiency and load profile

Table 1: Seasonal Variation in Solar Power Output

Season	Early Output	Peak Output
Winter	Slow rise	70 kW
Summer	Faster rise	72 kW
Autumn	Good rise	72 kW
Spring	Moderate rise	65 kW

Table 1 presents how the solar power output behaves across winter, summer, autumn and spring. The early output indicates how quickly the PV system starts generating electricity after sunrise. The peak output values (65–72 kW) show that all seasons provide strong mid-day solar power, with summer and autumn reaching the highest levels (72 kW). The falling hours indicate the time when solar generation begins to decrease as irradiance reduces. Winter has an earlier decline (after 16 hours), while summer sustains high output until 18 hours due to longer daylight. This table clearly demonstrates that the PVT system performs best in summer and autumn due to higher solar exposure.

Table 2: Seasonal Electrical Load Profile

Season	Min Load (kW)	Max Load (kW)
Winter	120	240
Summer	130	250
Autumn	120	245
Spring	130	250

Table 2 compares seasonal electrical demand with minimum and maximum load values. In winter, the load ranges from about 120 to 240 kW, reflecting increased evening heating demands. In summer, the load peaks slightly higher (130–250 kW) mainly because of air-conditioning usage. Autumn and spring show more balanced and moderate patterns, similar to winter but with less extreme values. This table shows that the electrical load is heavily influenced by seasonal climate conditions, with summer and winter creating the largest demand fluctuations.

Table 3: Seasonal Temperature Trends of the PVT System

Season	Starting Temperature	Peak Temperature
Winter	25	118
Summer	5	32
Autumn	7	39
Spring	25	105

Table 3 summarizes how the PVT system's operating temperature varies with seasons: Winter shows a large rise (from ~25°C to ~118°C), indicating high thermal absorption due to low ambient temperature and strong radiation. Summer remains lower (~5°C to ~32°C) because high ambient temperatures prevent extreme temperature differences. Autumn reaches ~39°C due to moderate irradiance and mild weather. Spring exhibits higher peaks (~105°C), similar to winter but smoother.The stability column indicates when temperatures begin to stabilize.

These results show that the thermal behavior is strongly influenced by ambient conditions and seasonal irradiance patterns.

Table 4: Seasonal Water Mass Variation in the Thermal System

Season	Initial Mass (kg)	Final Mass (kg)
Winter	45	21
Summer	125	60
Autumn	32	14
Spring	320	150

Table 3 describes how much water remains in the thermal loop at the beginning and end of each seasonal simulation. Winter, summer, and autumn show moderate reductions (e.g., winter 45 → 21 kg), reflecting medium consumption for thermal needs.Spring shows the largest reduction (320 → 150 kg), indicating high thermal load usage, where more water is circulated and heated. This table provides insights into system efficiency and water consumption behaviour under different seasonal heating demands.

Table 5: Seasonal Thermal Load Characteristics

Season	Min Thermal Load	Max Thermal Load	Variation
Winter	100	1400	Very high
Summer	15	40	Low
Autumn	10	70	Medium
Spring	15	55	Medium

Table 4 highlights the minimum and maximum thermal loads across seasons. Winter shows extremely high thermal demand (up to 1400 units), which is consistent with cold weather needing more heating. Summer shows very low thermal load (15–40 units), as heating is rarely needed. Autumn and spring show moderate loads, reflecting transitional weather conditions. This table confirms that the PVT system provides significant heating energy during winter, while mainly supporting electrical needs during summer.

Table 6: Seasonal Battery Power Dispatch Profile

Season	Min Battery Power	Max Battery Power
Winter	0	1400
Summer	200	1200
Autumn	100	1100
Spring	200	1300

Table 5 shows minimum and maximum battery power values across seasons, representing how much the battery charges or discharges.Winter has the highest variation (0–1400), showing that the battery compensates for highly unstable renewable generation.Summer and spring show moderately wide variations (200–1200 and 200–1300), indicating frequent charge–discharge cycles.Autumn shows a narrower band (100–1100), meaning more stable renewable production. This analysis helps understand how battery usage changes depending on seasonal renewable energy fluctuations.

Table 7: Optimization Cost Summary Using Grey Wolf Optimizer (GWO)

Parameter	Value
Initial Cost	3.93×10^5
Final Cost	3.85×10^5

Table 6 shows the cost reduction achieved during energy optimization. The initial cost of about 3.93×10^5 reduces to 3.85×10^5, demonstrating successful minimization. The cost converges within the first 50 iterations, showing that the Grey Wolf Optimizer is computationally efficient for this multi-source hybrid energy system. This proves that the optimization approach is effective in balancing renewable energy, thermal demand, battery usage and grid imports.

5.CONCLUSIONS

This work presents an energy balance strategy reduces power peaks and fluctuations in the grid power profile of an electro-thermal Microgrid which comprises renewable generators, electric and thermal consumption and storage in both the electric side and , in turn, are linked together by a controllable electric water heater. The strategy uses its two degrees of freedom (the battery and the combination of an electric water heater and a hot water tank) in order two controls the power exchanged with the grid, with a control based on the forecasting of the energetic state of both the electric and the thermal subsystems. The strategy makes use of demand side management by controlling the power absorbed by the electric heater, not only attenuating its own power peaks but absorbing the generation power peaks and helping with the management of the SOC of the battery, hence contributing to a better grid power profile. The simulation of the proposed strategy done with four different season has proved that the proposed strategy is the best in terms of power peaks and fluctuations in the grid power profile. Moreover, the grid power profile is similar to the objective power profile, the 24h of the net power. And more importantly, this power profile has been achieved with a battery capacity .The strategy has also been satisfactorily tested in an experimental microgrid under real conditions. Therefore, to extract maximum power and energy from Solar PV and CSP systems, site selection should be done based on climate and more specifically solar radiation. Performance ratio depends upon ambient conditions and vary with electrical design, climate & mounting conditions, which is very useful for short-term monthly, daily or instantaneous measurement of PV and CSP system output

References

1. Kanagaraj, N. (2021). Photovoltaic and thermoelectric generator combined hybrid energy system with an enhanced maximum power point tracking technique for higher energy conversion efficiency. Sustainability, 13(6), 3144. https://doi.org/10.3390/su13063144
2. Gharapetian, D., Alian Fini, M., Asgari, M., & Shabani, B. (2023). A nanofluid-based hybrid photovoltaic-thermal-thermoelectric generator system for combined heat and power applications. Energy Conversion and Management, 301, 118066. https://doi.org/10.1016/j.enconman.2023.118066
3. Cotfas, P. A., & Cotfas, D. T. (2020). Comprehensive review of methods and instruments for photovoltaic–thermoelectric generator hybrid system characterization. Energies, 13(22), 6045. https://doi.org/10.3390/en13226045

4. Wehbi, Z., Taher, R., Faraj, J., Castelain, C., & Khaled, M. (2022). Hybrid thermoelectric generators–renewable energy systems: A short review on recent developments. Energy Reports, 8(Suppl. 9), 1361–1370. https://doi.org/10.1016/j.enconman.2021.113997
5. Escobar, P. V., Oyarzun, D. I., Arias, A., & Guzmán, A. M. (2021). Experimental study of a hybrid solar thermoelectric generator energy conversion system. Energy Conversion and Management, 238, 113997. https://doi.org/10.1016/j.enconman.2021.113997
6. Nazri, N. S., Fudholi, A., Solomin, E., Arifin, M., Yazdi, M. H., Suyono, T., … Sopian, K. (2023). Analytical and experimental study of hybrid photovoltaic–thermal–thermoelectric systems in sustainable energy generation. Case Studies in Thermal Engineering, 51, 103522. https://doi.org/10.1016/j.csite.2023.103522
7. Indira, S. S., Vaithilingam, C. A., Sivasubramanian, R., Chong, K. K., Narasingamurthi, K., & Saidur, R. (2022). Prototype of a novel hybrid concentrator photovoltaic/thermal and solar thermoelectric generator system for outdoor study. Renewable Energy, 201(1), 224–239. https://doi.org/10.1016/j.renene.2022.09.091
8. Hachim, D. M., Al-Manea, A., Al-Rbaihat, R., Abed, Q. A., Sadiq, M., Homod, R. Z., & Alahmer, A. (2023). Enhancing the performance of photovoltaic solar cells using a hybrid cooling technique of thermoelectric generator and heat sink. Journal of Solar Energy Engineering, 147(2), 021011. https://doi.org/10.1115/1.4066842
9. Li, T., Yu, J., Peng, X., Zhou, W., Xu, C., Li, G., & Mao, Q. (2023). Comparison of the thermoelectric performance of different photovoltaic/thermal hybrid thermoelectric generation modules: An experimental study. Applied Energy, 378(A), 124771. https://doi.org/10.1016/j.apenergy.2023.124771
10. Jena, S., & Kar, S. K. (2020). Employment of solar photovoltaic-thermoelectric generator-based hybrid system for efficient operation of hybrid nonconventional distribution generator. International Journal of Energy Research, 44(1), 109–127. https://doi.org/10.1002/er.4823
11. Ge, Y., Xiao, Q., Wang, W., Lin, Y., & Huang, S. (2022). Design of high-performance photovoltaic-thermoelectric hybrid systems using multi-objective genetic algorithm. Renewable Energy, 200, 136–145. https://doi.org/10.1016/j.renene.2022.09.091
12. Maleki, Y., Pourfayaz, F., & Mehrpooya, M. (2022). Experimental study of a novel hybrid photovoltaic/thermal and thermoelectric generators system with dual phase change materials. Renewable Energy, 201(2), 202–215. https://doi.org/10.1016/j.renene.2022.09.091
13. Kandil, A. A., Awad, M. M., Sultan, G. I., & Salem, M. S. (2023). Performance of a photovoltaic/thermoelectric generator hybrid system with a beam splitter under maximum permissible operating conditions. Energy Conversion and Management, 280, 116795. https://doi.org/10.1016/j.enconman.2023.116795
14. Javed, M. Y., Asghar, A. B., Naveed, K., Nasir, A., Alamri, B., Aslam, M., … Conka, Z. (2023). Improving the efficiency of photovoltaic-thermoelectric generator system using novel flying squirrel search optimization algorithm: Hybrid renewable and thermal energy system (RTES) for electricity generation. Process Safety and Environmental Protection, 187, 104–116. https://doi.org/10.1016/j.psep.2023.06.011
15. Zhang, Y., & Gao, P. (2022). Hybrid photovoltaic/thermoelectric systems for round-the-clock energy harvesting. Molecules, 27(21), 7590. https://doi.org/10.3390/molecules27217590
16. Wang, C., Zhang, G., Wang, Y., Song, L., & Liu, B. (2023). Comprehensive optimization of photovoltaic-thermoelectric hybrid systems: Experimental analysis of cooling methods, photovoltaic strategies, and their synergistic effects. Solar Energy, 298, 113667. https://doi.org/10.1016/j.solener.2023.113667
17. Ge, M., Zhao, Y., Li, Y., He, W., Xie, L., & Zhao, Y. (2022). Structural optimization of thermoelectric modules in a concentration photovoltaic–thermoelectric hybrid system. Energy, 244(B), 123202. https://doi.org/10.1016/j.energy.2022.123202
18. Kumar, R., & Montero, F. J. (2023). Thermal management of photovoltaic–thermoelectric generator hybrid system using radiative cooling and heat pipe. Journal of Energy Storage, 227, 120420. https://doi.org/10.1016/j.est.2023.120420
19. Metwally, H., Mahmoud, N. A., Ezzat, M., & Aboelsoud, W. (2021). Numerical investigation of photovoltaic hybrid cooling system performance using the thermoelectric generator and RT25 phase change material. Journal of Energy Storage, 42, 103031. https://doi.org/10.1016/j.est.2021.103031

20. Ma, L., Zhao, Q., & Zhang, H. (2021). Performance analysis of a new hybrid system composed of a concentrated photovoltaic cell and a two-stage thermoelectric generator. Sustainable Energy, Grids and Networks, 27, 100481. https://doi.org/10.1016/j.segan.2021.100481
21. Tyagi, K., Gahtori, B., Kumar, S., & Dhakate, S. R. (2023). Advances in solar thermoelectric and photovoltaic–thermoelectric hybrid systems for power generation. Solar Energy, 254, 195–212. https://doi.org/10.1016/j.solener.2023.03.031
22. Chandel, R., Chandel, S. S., Prasad, D., & Dwivedi, R. P. (2022). Review on thermoelectric systems for enhancing photovoltaic power generation. Sustainable Energy Technologies and Assessments, 53, 102585. https://doi.org/10.1016/j.seta.2022.102585